

See discussions, stats, and author profiles for this publication at: <https://www.researchgate.net/publication/262488471>

# Synthesis of novel 2-mercaptobenzoxazole based 1,2,3-triazoles as inhibitors of proinflammatory cytokines and suppressors of COX-2 gene expression

ARTICLE · MAY 2014

---

READS

61

1 AUTHOR:



Saqlain Haider

University of Mississippi

30 PUBLICATIONS 69 CITATIONS

SEE PROFILE



## Original article

# Synthesis of novel 2-mercaptobenzoxazole based 1,2,3-triazoles as inhibitors of proinflammatory cytokines and suppressors of COX-2 gene expression



Saqlain Haider <sup>a</sup>, Mohammad Sarwar Alam <sup>a,\*</sup>, Hinna Hamid <sup>a</sup>, Syed Shafi <sup>a</sup>,  
Abhijeet Dhulap <sup>c</sup>, Firasat Hussain <sup>b</sup>, Pervez Alam <sup>d</sup>, Sadiq Umar <sup>e</sup>, M.A.Q. Pasha <sup>d</sup>,  
Sameena Bano <sup>a</sup>, Syed Nazreen <sup>a</sup>, Yakub Ali <sup>a</sup>, Chetna Kharbanda <sup>a</sup>

<sup>a</sup> Department of Chemistry, Faculty of Science, Jamia Hamdard (Hamdard University), New Delhi 110 062, India

<sup>b</sup> Department of Chemistry, Faculty of Science, University of Delhi, New Delhi 110007, India

<sup>c</sup> Unit for Research and Development of Information Products – CSIR, Pune 411038, India

<sup>d</sup> Functional Genomics Unit, CSIR – Institute of Genomics & Integrative Biology, New Delhi 110007, India

<sup>e</sup> Department of Toxicology, Faculty of Science, Jamia Hamdard (Hamdard University) New Delhi 110 062, India

## ARTICLE INFO

## Article history:

Received 21 January 2014

Received in revised form

5 April 2014

Accepted 2 May 2014

Available online 4 May 2014

## Keywords:

Cyclooxygenase



Molecular docking

Antinociceptive

Gene expression

## ABSTRACT

A library of novel bis-heterocycles containing 2-mercaptobenzoxazole based 1,2,3-triazoles has been synthesized using click chemistry approach. The compound **4** exhibited the most potent *in vivo* anti-inflammatory activity with 66.66% and 61.11% inhibition in comparison to celecoxib which showed 72.22% and 65.55% inhibition after 3 h and 5 h respectively. The compounds **4** and **9** suppressed the COX-2 gene expression by 0.94 and 0.79 fold and exhibited a selective index (COX-1/COX-2) of 64.79 and 66.47 respectively in comparison to celecoxib (SI value of 75.56). The *in silico* molecular docking studies showed the interactions of these molecules with Tyr-59, Tyr-119 and Gly-121. When compared with the standard drug celecoxib, compounds **4**, **5**, **7**, **9** and **16** did not cause any gastric ulceration.

© 2014 Elsevier Masson SAS. All rights reserved.

## 1. Introduction

The present market of the anti-inflammatory drugs is encumbered with NSAIDs associated with adverse effects like ulceration and gastric haemorrhage [1]. A prolonged consumption of these drugs may cause gastric injuries [2]. The pro-inflammatory mediators like TNF- $\alpha$ , IL-1 $\beta$ , NO and COX-2 play an imperative role in the inflammatory reactions like tissue destruction, shock and organ failure [3–5]. The aim of this work is to develop new molecules with a potential to inhibit the increase in the level of proinflammatory mediators such as TNF- $\alpha$ , IL-1 $\beta$ , NO and COX-2 without inducing any gastric ulceration. Our group has recently reported the 2-mercaptobenzothiazole based 1,2,3-triazoles as a class of anti-inflammatory and antinociceptive agents with potent COX-2

selectivity [6]. This prompted us to synthesize and evaluate the anti-inflammatory activity (Fig. 1) of 2-mercaptobenzoxazole based 1,2,3-triazoles which has an oxygen atom in place of the sulphur atom in the benzoxazole nucleus.

2-mercaptobenzoxazoles are the thiol derivatives (Fig. 2) of simple benzoxazole nucleus. They exist in two tautomeric forms i.e. thiol and thione [7].

2-mercaptobenzoxazoles have emerged as a potent medicinal scaffold and have remained the focus of drug discovery due to their important therapeutic values [8]. Benzoxazoles and their derivatives are known to exhibit antibacterial, antifungal, antitumour, anti-tubercular, anti-inflammatory and HIV-1 reverse transcriptase inhibitory activities [9–13]. 1,2,3-triazole nucleus is present in many drugs [14] and has been found to be associated with potent antimicrobial [15,16], anti-inflammatory [17], local anaesthetic [18], anticonvulsant [19], anti-neoplastic [20], antimalarial [21] and antiviral activities [22]. In continuation of our efforts to develop novel molecules for the treatment of inflammatory disorders like

\* Corresponding author.

E-mail addresses: [msalam@jamiahAMD.ac.in](mailto:msalam@jamiahAMD.ac.in), [msalam5555@gmail.com](mailto:msalam5555@gmail.com) (M.S. Alam).



**Fig. 1.** The structural resemblance of 2-mercaptopbenzoxazole with 2-mercaptopbenzothiazole is shown.

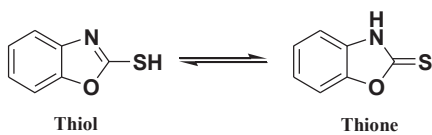


**Fig. 2.** The tautomeric forms of 2-mercaptopbenzoxazole are shown.

osteoarthritis and crohn's disease we have linked the 1,2,3-triazole nucleus with 2-mercaptopbenzoxazoles under one construct through a methylene linkage. We have carried out the *in silico* molecular docking studies with respect to COX-2 and TNF- $\alpha$  target in order to get an insight into the binding modes of these novel molecules with their active sites. The compounds showing significant *in vivo* anti-inflammatory activity have been further screened against proinflammatory cytokine mediators like TNF- $\alpha$ , IL-1 $\beta$ , COX-2 and NO using *in vivo* assays. The potent anti-inflammatory molecules thus obtained were subjected to *in vivo* antinociceptive activity by writhing test method followed by their gastric ulceration study. It was observed that the compounds **4**, **5**, **7**, **9** and **16** did not induce any gastric ulceration. Since the free radical production occurs simultaneously during inflammation therefore we have screened our compounds for their antioxidant activity using reduced glutathione and lipid peroxidation assays.

## 2. Results and discussion

### 2.1. Chemistry

A focused library of eighteen novel compounds has been synthesized. As shown in Scheme 1, 2-mercaptopbenzoxazole on being refluxed with propargyl bromide and potassium carbonate in dry acetone for 5–7 h yielded the propargyl derivative (**A**). The 1,3-dipolar cycloaddition of the propargylated 2-mercaptopbenzoxazole derivative (**A**) with different substituted aromatic azides under click chemistry conditions resulted in the formation of novel 2-mercaptopbenzoxazole based 1,2,3-triazoles (**1–18**) in quantitative yields (Table 1). Aromatic azides with various substitutions including electron withdrawing and electron donating groups have been used. The propargylation of the 2-mercaptopbenzoxazole was confirmed by the presence of a signal in a range of  $\delta$  4.76–4.81 (s, 2H,

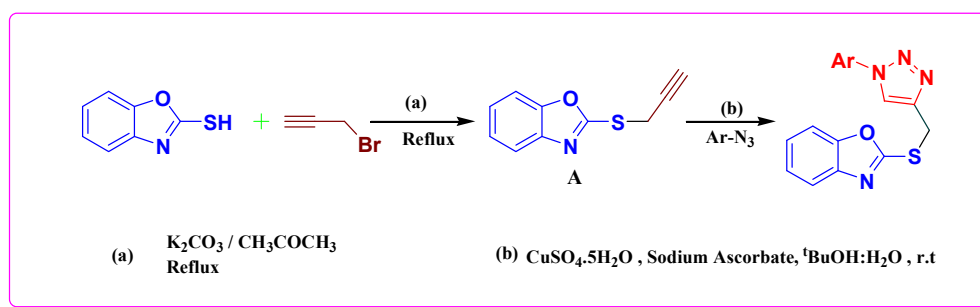
CH<sub>2</sub>) in the <sup>1</sup>H NMR spectra. The formation of 1,2,3-triazoles was confirmed by the resonance of the triazolyl proton as singlet in a range of  $\delta$  8.29–8.91 for different derivatives. The structural assignment was also supported by the <sup>13</sup>C NMR spectral data, which showed the C-atom signals corresponding to triazole derivatives. The final confirmation was made by the ESI-MS analysis which showed the presence of [M]<sup>+</sup> or [M+1]<sup>+</sup> or [M+2]<sup>+</sup> or [M+3]<sup>+</sup> ion peaks. Compound **6** was also subjected to X-ray crystallographic study which is being reported here for the first time.

### 2.2. *In vivo* anti-inflammatory activity

All the synthesized compounds have been screened for their *in vivo* anti-inflammatory activity by the carrageenan-induced hind paw edema model. All the compounds showed a time-dependent decrease in the inhibition of inflammation after 3 h and 5 h. It was found that the compound **4** showed potent anti-inflammatory activity with 66.66% and 61.11% inhibition after 3 h and 5 h as compared to celecoxib which showed 72.22% and 65.55% inhibition after 3 h and 5 h respectively (Fig. 3). The compound **7** exhibited 68.88% inhibition at 3 h post-carrageenan and 55.55% inhibition, 5 h post-carrageenan administration in comparison to celecoxib. It was observed that the compounds **5**, **9** and **16** exhibited moderate anti-inflammatory activity in comparison to the standard drug celecoxib.

### 2.3. Effect on IL-1 $\beta$ , TNF- $\alpha$ and COX-2

During the inflammatory reactions, large amounts of the proinflammatory mediators are generated which affect the immune system by suppressing the proliferation of T and B cells, as well as cytokine synthesis [23]. Blockade of these molecules results in a reduction of disease severity and bone resorption [24–27]. Proinflammatory cytokines like IL-1 $\beta$  and TNF- $\alpha$  as well as COX-2 have an important role in the perpetuation of chronic inflammation and tissue damage during progression of inflammatory disorder. There is a significant increase in the level of TNF- $\alpha$ , IL-1 $\beta$  and COX-2 in carrageenan induced edema rats as compared to the control (Fig. 4). Administration of the selected active compounds **4**, **5**, **7**, **9** and **16** suppressed the increase in the level of IL-1 $\beta$ , TNF- $\alpha$  and COX-2 significantly when compared with the edema group. The compound **16** exhibited a reduction in the level of IL-1 $\beta$  to  $2.66 \pm 0.13$  pg/ml in comparison to celecoxib which showed a reduction to  $2.90 \pm 0.16$  pg/ml. The compound **5** suppressed the level of TNF- $\alpha$  to  $3.10 \pm 0.17$  pg/ml in comparison to celecoxib which showed a reduction to  $3.35 \pm 0.16$  pg/ml. A significant decrease in the amount of COX-2 was also observed for the compound **5** which reduced the COX-2 level to  $6.54 \pm 0.26$  as compared to celecoxib which showed a reduction to  $7.90 \pm 0.25$ . The compounds **4** (COX-1 IC<sub>50</sub> = 246.20  $\mu$ M; COX-2 IC<sub>50</sub> = 3.8  $\mu$ M; SI = 64.79) and **9** (COX-1 IC<sub>50</sub> = 186.11  $\mu$ M;



**Scheme 1.** Synthesis of novel 2-mercaptopbenzoxazole linked 1,2,3-triazoles.

**Table 1**

Structures of the novel 2-mercaptobenzoxazole based 1,2,3-triazole.

Compound	% Yield	Structure
1	85	
2	88	
3	90	
4	88	
5	92	
6	94	
7	90	
8	88	
9	86	
10	92	
11	83	
12	86	

**Table 1 (continued)**

Compound	% Yield	Structure
13	90	
14	88	
15	88	
16	85	
17	84	
18	85	

COX-2 IC<sub>50</sub> = 2.8 μM; **SI** = 66.47) exhibited potent selective COX-2 inhibition as compared to celecoxib (COX-1 IC<sub>50</sub> = 20.40 μM; COX-2 IC<sub>50</sub> = 0.27 μM; **SI** = 75.56). The gastric tolerance of these compounds may be related to their selective COX-2 inhibition (**Table 2**).

The structure activity relationship of the synthesized compounds has been analysed on the basis of **COX-1/COX-2** ratio (Selective Index). The **SI** values were found to vary depending upon the nature and the position of the substituents on the aryl ring attached with the 1,2,3-triazole ring. The compounds containing electron donating groups on the *para* position of the aryl ring exhibited more potent anti-inflammatory activity in comparison to the compounds containing electron withdrawing groups. The compounds **4**, **16** and **15** containing the C<sub>2</sub>H<sub>5</sub>, OC<sub>2</sub>H<sub>5</sub> and C(CH<sub>3</sub>)<sub>3</sub> groups respectively at the *para* position displayed potent selectivity towards COX-2 with the **SI** values of 64.79, 46.64 and 40.06 respectively. The **COX-2** selectivity was considerably reduced by the presence of the strong electron withdrawing NO<sub>2</sub> group at the *meta* (**SI** = 10.80) and *para* (**SI** = 11.67) positions for the compounds **1** and **2** respectively.

Amongst the halogen containing compounds the **COX-2** selectivity was found to decrease with a decrease in the size of halogen (Br > Cl > F) i.e. activity was found to decrease in the order **9**(**SI** = 66.47) > **7**(**SI** = 42.54) > **10**(**SI** = 36.88). The *para* substituted halogen containing compounds **7**, **9**, and **10** were found to exhibit more potent **COX-2** selectivity in comparison to their corresponding *ortho* substituted derivatives i.e. **8**, **12** and **13**. The compounds **17** and **18** containing pyridyl and substituted pyridyl ring, respectively exhibited a moderate **COX-2** selectivity with a selectivity index of 24.26 and 20.40.

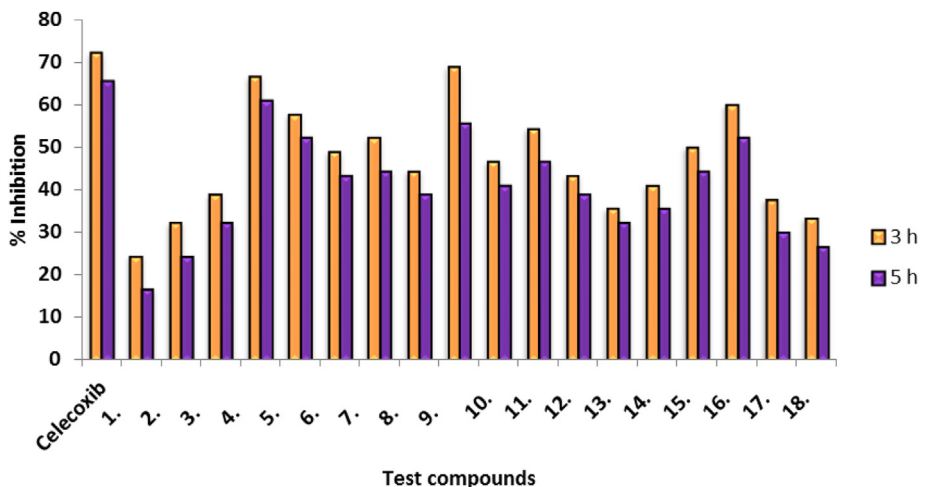


**Fig. 3.** The results of the *in vivo* antiinflammatory activity of all the synthesized compounds by carrageenan induced hind paw edema method is shown.

#### 2.4. Gene expression study on COX-2

The results of the gene expression study on COX-2 (Fig. 5) showed that the compounds **4** and **9** suppressed the expression of

COX-2 gene by 0.94 and 0.79 fold in comparison to the standard drug celecoxib. Thus these molecules may be used to develop new leads for the treatment of inflammatory disorders like arthritis.

#### 2.5. Nitric oxide

Nitric oxide (NO) is an important signalling molecule, produced as part of the inflammatory response from activated cells and macrophages [28,29]. An increase in the NO level has been previously reported in synovial fluids of patients suffering from rheumatoid arthritis [30]. In the present study, increased NO levels have been detected in carrageenan group similar to those previously reported in synovial fluids of patients with rheumatoid arthritis. Analysis of nitrite estimation is summarised in Fig. 6. A significant increase in the nitrite level was observed in carrageenan induced edema group as compared to control. All synthesized compounds declined the increase in the nitrite level significantly as compared to the edema group. Compound **4** significantly suppressed the increase in the NO level to  $5.10 \pm 0.18 \mu\text{mol}/\text{mg}$  comparison to celecoxib which showed a reduction to  $5.50 \pm 0.16 \mu\text{mol}/\text{mg}$ .

#### 2.6. Effect on TBARS and GSH

Lipid peroxidation has been implicated in the pathogenesis of cancer, atherosclerosis, degenerative diseases and inflammatory arthritis [31]. During lipid Peroxidation, lipid peroxyl radicals are produced that cause cell membrane damage. Matrix degradation arising from cytokine-stimulated chondrocytes has been shown to be primarily due to lipid peroxidation [32]. The effect of all the synthesized compounds on TBARS (Thiobarbituric acid reactive substances) level was measured to demonstrate the oxidative damage on lipid Fig. 7. A significant increase in TBARS level was observed in carrageenan induced edema group when compared to the control group. The level of TBARS was suppressed to  $5.10 \pm 0.23 \text{ nmole}$  by the compound **16** whereas celecoxib reduced the TBARS level to  $6.3 \pm 0.16 \text{ nmole}$ . Free radical production that occurs during development of arthritis in the articular cartilage leads to decreased GSH (Glutathione) and SOD (Super oxide dismutase) levels as a result of their consumption during oxidative stress and cellular lysis [33–35]. The concentration of GSH was evaluated to estimate endogenous defences against hydrogen peroxide formation. Fig. 8 shows the changes in GSH levels evaluated in the joints of the experimental groups. A marked decrease in GSH was found in the hind paw joint of carrageenan induced ( $0.58 \pm 0.020 \mu\text{GSH/g tissue}$ ) edema rats. However the treatment

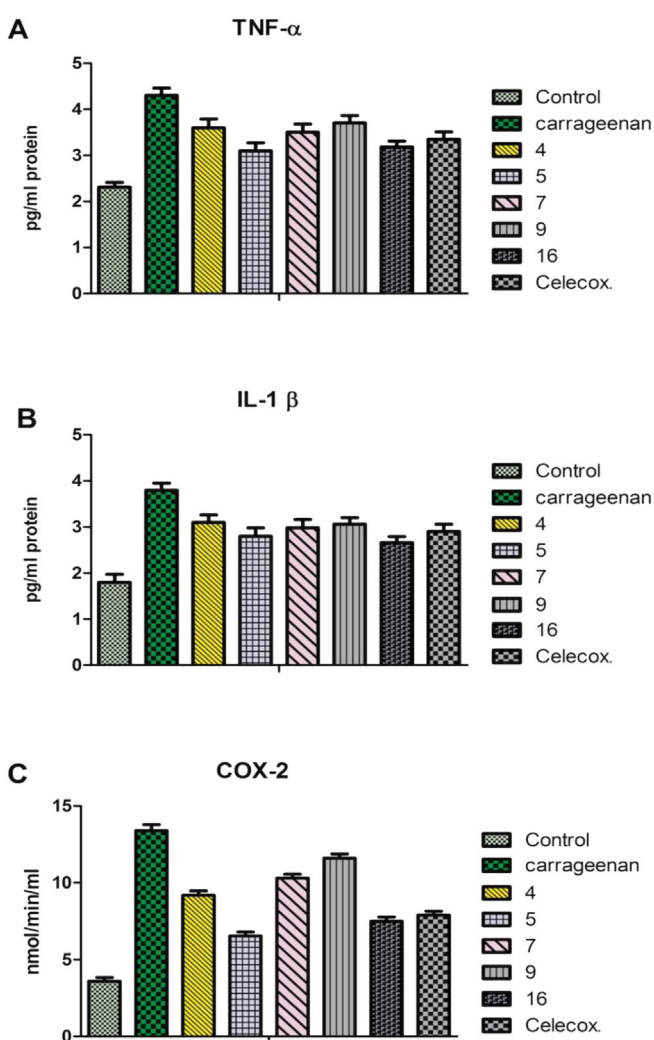


**Fig. 4.** The compounds **4**, **5**, **7**, **9** and **16** showing potent *in vivo* antiinflammatory activity have been screened for their effects on the levels of the TNF- $\alpha$ , IL-1 $\beta$  and COX-2 in the serum.

**Table 2**

Inhibitory activity of the 1,2,3-triazole based benzoxazolinones.

Compounds	IC <sub>50</sub> (μM)		Selectivity index COX-1/COX-2
	(COX-1)	(COX-2)	
<b>1</b>	103.52	9.58	10.80
<b>2</b>	115.23	9.87	11.67
<b>3</b>	107.25	6.42	16.70
<b>4</b>	<b>246.20</b>	<b>3.8</b>	<b>64.79</b>
<b>5</b>	89.37	2.3	38.86
<b>6</b>	88.26	4.63	19.06
<b>7</b>	<b>80.82</b>	<b>1.9</b>	<b>42.54</b>
<b>8</b>	44.35	3.53	12.56
<b>9</b>	<b>186.11</b>	<b>2.8</b>	<b>66.47</b>
<b>10</b>	192.15	5.21	36.88
<b>11</b>	132.32	4.68	28.27
<b>12</b>	38.36	2.75	13.94
<b>13</b>	24.23	2.40	10.09
<b>14</b>	140.45	4.35	32.28
<b>15</b>	<b>154.26</b>	<b>3.85</b>	<b>40.06</b>
<b>16</b>	<b>163.24</b>	<b>3.5</b>	<b>46.64</b>
<b>17</b>	96.56	3.98	24.26
<b>18</b>	102.66	5.03	20.40
Celecoxib	<b>20.40</b>	<b>0.27</b>	<b>75.56</b>

Values are the means ± SEM from three independent experiments using COX assay kits (Cayman Chemicals Inc., Ann Arbor, MI, USA). The bold values signify the most potent molecules in the given list.

with compounds **4** ( $0.84 \pm 0.025 \mu\text{GSH/g tissue}$ ) and **16** ( $0.84 \pm 0.027 \mu\text{GSH/g tissue}$ ) significantly inhibited the decrease in GSH as compared to celecoxib ( $0.81 \pm 0.027 \mu\text{GSH/g tissue}$ ).

### 2.7. Molecular docking studies on COX-2

In order to get an insight into the binding mode of the synthesized molecules with COX-2, all the newly synthesized molecules have been docked against COX2 (PDB NO: 3LN1). All the molecules were docked against COX-2 target protein separately. Fig. 9a and b show that the compounds **4** and **9** have purely hydrophobic interactions with the COX-2 protein. The binding energies of the eighteen new ligands were found to be in a range of  $-23.07$  to  $-48.4$  kcal/mol. Compounds **4** (G score = **-8.6**) and **9** (G score = **-8.14**) were found to have the closest binding efficiency with respect to celecoxib (G score = **-11.29**). The predicted binding energies are summarized in Table 3. The QikProp program was used to predict the ADME (absorption, distribution, metabolism and excretion) properties of the molecules. Normal mode was applied in the program to predict the partition coefficient ( $\log P_{\text{o/w}}$ ), van der Waals surface area of polar nitrogen and oxygen atoms (PSA) and aqueous solubility ( $\log S$ ) properties. The results obtained are listed in Table 4 respectively. As seen from the table the values of the calculated properties are within the acceptable range.

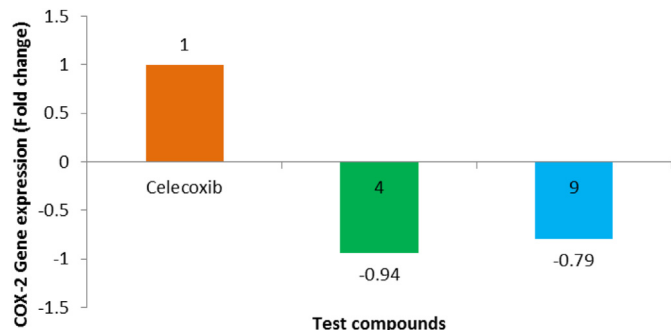


Fig. 5. The compounds **4** and **9** suppressed the COX-2 gene expression by 0.94 and 0.79 folds respectively.

### 2.8. Molecular docking studies on TNF-α

The binding pocket of 2AZ5 is large and without defined cervices. The binding site is mainly hydrophobic consisting of glycine, leucine and tyrosine residues. In order to bind to this hydrophobic large pocket, the ligands also need to be hydrophobic and of large size. Before docking the new ligands against the generated grid, the reference ligand was separately docked against the generated grid to validate the grid and docking methodology. Fig. 10a shows comparison between the original binding modes of reference ligand against docked binding mode as predicted by Schrodinger Glide software. Fig. 10a clearly shows that adapted Schrodinger methodology successfully predicted the binding mode with root mean square deviation of  $0.003 \text{ \AA}$ . All the ligands were docked against TNF-α target protein separately. Fig. 10b and c shows that the compound **8** is embedded in the pocket of the TNF-α protein and compound **10** is involved in H-bond formation with GLY 121 residue. The binding energies of the eighteen novel ligands was found to be in the range of  $-35.09$  to  $-41.4$  kcal/mol. Molecules **8** (G score = **-6.38**) and **10** (G score = **-6.77**) exhibited the closest binding efficiency with respect to reference ligand 2AZ5 (G score = **-7.1**). The predicted binding energies are summarized in Table 5. The QikProp program was used to predict the ADME (absorption, distribution, metabolism and excretion) properties of the molecules. Normal mode was applied in the program to predict partition coefficient ( $\log P_{\text{o/w}}$ ), van der Waals surface area of polar nitrogen and oxygen atoms (PSA) and aqueous solubility ( $\log S$ ) properties. The results obtained are listed in Table 6. As seen from the table the values of the calculated properties lie within the acceptable range.

### 2.9. In vivo antinociceptive activity

The compounds showing significant *in vivo* anti-inflammatory activity have been further evaluated for their *in vivo* antinociceptive potential. It was found that the compounds **5** and **7** exhibited 55.55% and 51.50% inhibition (Fig. 11) respectively in comparison to celecoxib which showed 70.89% inhibition.

### 2.10. Ulcerogenic study

The compounds showing potential *in vivo* anti-inflammatory and *in vivo* antinociceptive activities were further tested for their gastric ulceration activity (Fig. 12). When compared with celecoxib, the compounds **4**, **5**, **7**, **9** and **16** did not induce any gastric ulceration and rupture of the gastric mucosal layer.

### 2.11. Crystallographic study

Intensity data were collected at  $183(2)$  K an Oxford Xcalibur Sapphire 3 diffractometer (a single wavelength Enhance X-ray source with  $\text{MoK}_\alpha$  radiation,  $\lambda = 0.71073 \text{ \AA}$ ) [36]. The selected suitable single crystals were mounted using paratone oil on the top of a glass fiber fixed on a goniometer head and immediately transferred to the diffractometer. Pre-experiment data collection, data reduction and analytical absorption corrections [37] were performed with the Oxford program suite [38] CrysAlisPro. The crystal structures were solved with SHELLXS-97 [38] using direct methods. The structure refinements were performed by full-matrix [39] least-squares on  $P^2$  with SHELLXL-97. All programs used during the crystal structure determination process were present in the WINGX software [40]. The chemical formula and ring labelling system is shown in Fig. 13. Crystal data for compound **6**:  $\text{C}_{16}\text{H}_{11}\text{ClN}_4\text{OS}$ , Mr, 342.80; system, triclinic; space group, P-1; unit cell dimensions,  $a = 6.7407(3) \text{ \AA}$ ;  $b = 7.4806(5) \text{ \AA}$ ;  $c = 15.6537(9)$

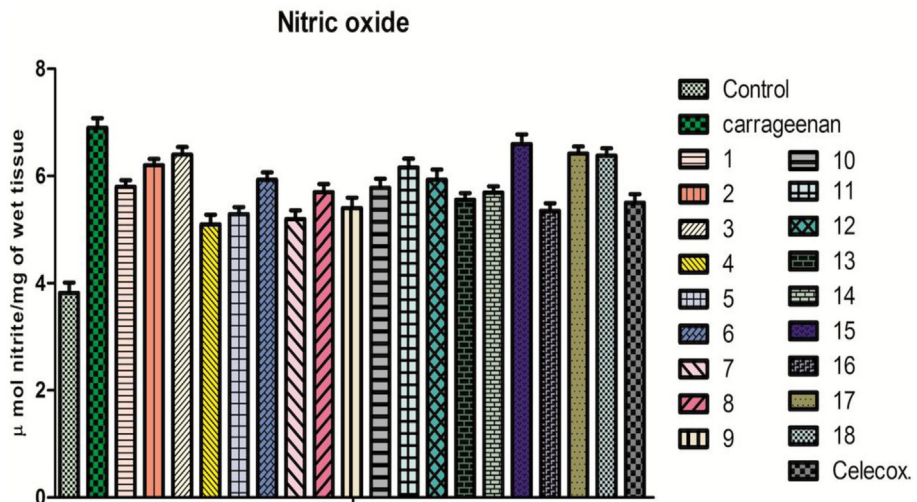


**Fig. 6.** All the synthesized compounds have been screened for their effect on the level of Nitric oxide.

$\text{\AA}$ ;  $\alpha = 78.181$  (5) $^\circ$ ;  $\beta = 79.697$  (4) $^\circ$ ;  $\gamma = 82.127$  (5) $^\circ$ ;  $V = 756.00$  (7) $\text{\AA}^3$ ;  $Z = 2$ ;  $T = 298$  K;  $R_{\text{int}} = 0.0380$ ;  $R$  (all), 0.0442;  $Gof = 1.076$ ;  $\Delta\rho_{\text{max}} = 0.23$  e  $\text{\AA}^3$ ;  $\Delta\rho_{\text{min}} = -0.35$  e  $\text{\AA}^3$ . All hydrogen atoms were calculated after each cycle of refinement using a riding model, with  $\text{C}-\text{H} = 0.93\text{\AA} + U_{\text{iso}}(\text{H}) = 1.2U_{\text{eq}}(\text{C})$  for aromatic H atoms, with  $\text{C}-\text{H} = 0.97\text{\AA} + U_{\text{iso}}(\text{H}) = 1.2U_{\text{eq}}(\text{C})$  for methylene H atoms. Crystallographic data for the compound **6** has been deposited with the Cambridge Crystallographic Data Center (CCDC) under the number 950223. Copies of the data can be obtained, free of charge, on application to CCDC 12 Union Road, Cambridge CB2 1EZ, UK [Fax: þ44-1223-336033; e-mail: [deposit@ccdc.cam.ac.uk](mailto:deposit@ccdc.cam.ac.uk) or at [www.ccdc.cam.ac.uk](http://www.ccdc.cam.ac.uk)].

### 3. Conclusion

We have synthesized a focussed library of novel bis-heterocycles containing 2-mercaptopbenzoxazole moiety and 1,2,3-triazole nucleus conjugated through a methylene linkage. The crystallographic study of the compound **6** confirmed the formation of final molecule and supported the spectroscopic data. The compounds **4**, **5**, **7**, **9** and **16** exhibiting potent *in vivo* anti-inflammatory and *in vivo*

antinociceptive activities have been further screened for their *in vivo* COX-2 selectivity and proinflammatory cytokine mediators like TNF- $\alpha$ , IL-1 $\beta$  and NO. The results of the *in vivo* (COX 1/COX-2) selective index showed that the compounds **4** and **9** exhibit a target specific inhibitor of COX-2, which is comparable with the standard drug celecoxib. The compounds **4** and **9** suppressed the COX-2 gene expression by 0.94 and 0.79 fold which in turn shows their potential to reduce inflammation by inhibiting the expression of COX-2 gene. The results of the *in silico* molecular docking studies against COX-2 showed that hydrogen bonding and hydrophobic interactions are responsible for the interactions of the synthesized compounds with their corresponding active sites on the target protein. The *in silico* molecular docking study against TNF- $\alpha$  shows that the molecule **8** interacts with Tyr-59 and Tyr-119 amino acid residues on the TNF- $\alpha$  protein. The molecule **10** was found to show the interactions with Tyr-59 and Gly-121 on TNF- $\alpha$  protein. The compounds **4**, **5**, **7**, **9** and **16** did not induce any gastric ulceration thus showing their effective tolerance towards gastric mucosa. Thus these molecules may be used as leads for the development of novel anti-inflammatory drugs which may help in the treatment of inflammatory disorders like rheumatoid arthritis and crohn's disease.

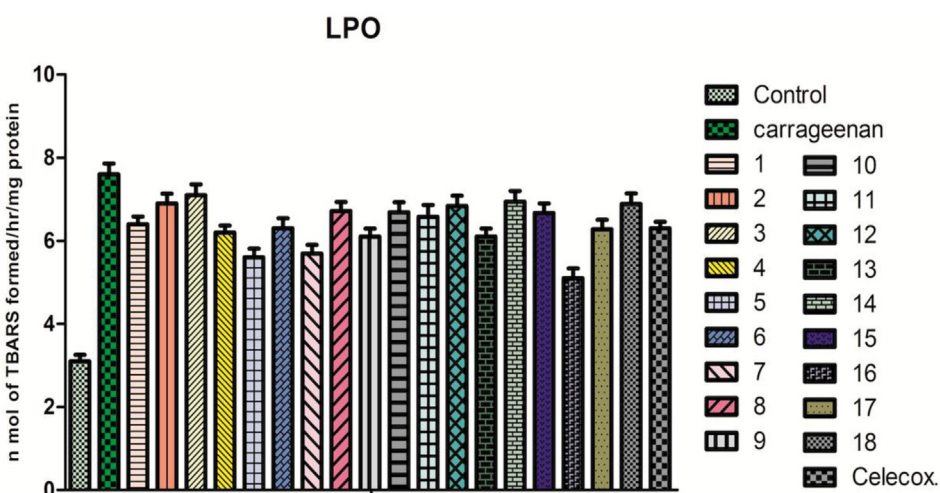


**Fig. 7.** The results the antioxidant activity by the lipid peroxidation are shown.

### Reduced Glutathione



**Fig. 8.** The results the antioxidant activity by the glutathione method are shown.

## 4. Experimental

### 4.1. Chemistry

All the chemicals and reagents used in this study were purchased from Merck (India), Spectrochem and Sigma Aldrich. All melting points were uncorrected and measured using Veego VMP-DS apparatus, IR spectra were recorded as potassium bromide pellets on a Perkin Elmer 1650 spectrophotometer (USA), 1H NMR spectra was determined on a Bruker (200, 300 and 400 MHz) spectrometer and chemical shifts were expressed as ppm against

TMS as internal reference. Mass spectra were recorded on 70 eV (EI Ms-QP 1000EX, Shimadzu, Japan) and Column Chromatography was performed on (Merck) Silica gel 60 (particle size 0.06e 0.20 mm). All compounds prepared in this paper are novel and their formation has been confirmed from the spectral data. Compound **A** obtained from the propargylation of 2-mercaptopbezoxazole was dissolved in 20 mL of <sup>1</sup>Butanol:water (1:1) solvent at ambient temperature. CuSO<sub>4</sub>.5H<sub>2</sub>O was charged into it and the reaction mixture was stirred for 5 min at the room temperature. Reaction mixture became light blue in colour. Then sodium ascorbate was added to the reaction mixture and stirred for 15 min. The colour of

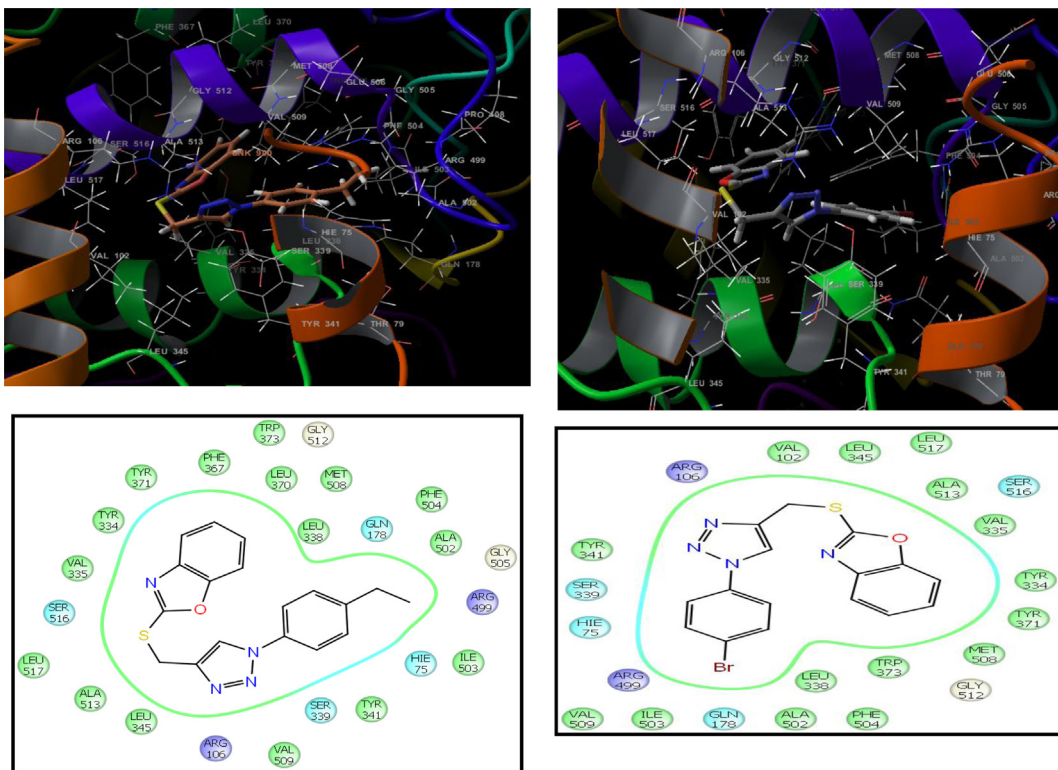


**Fig. 9.** a: The *in silico* molecular docking structure of the compound **4** against COX-2 protein is shown. b: The *in silico* molecular docking structure of the compound **9** against COX-2 protein is shown.

**Table 3**

*In silico* docking scores of celecoxib and 18 new ligands with respect to COX-2 protein.

Ligand	G Score	Glide energy
Celecoxib	-11.29	-61.11
4	<b>-8.6</b>	<b>-45.46</b>
9	<b>-8.14</b>	<b>-47.29</b>
6	<b>-8.08</b>	<b>-27.08</b>
14	<b>-8.05</b>	<b>-28.72</b>
8	-7.77	-29.1
2	-7.72	-48.46
11	-7.7	-30.55
13	-7.69	-39.88
16	-7.65	-41.56
10	-7.63	-36.39
17	-7.48	-41.89
18	-7.43	-38.94
3	-7.41	-28.36
5	-7.41	-41.44
12	-7.34	-28.72
1	-7.15	-36.25
15	-5.75	-23.07

The bold values signify the most potent molecules in the given list.

the reaction mixture then changed to dark yellow. After 15 min azides were added. The reaction mixture was then allowed to stir for further 5–7 h at ambient temperature. After the completion of the reaction, monitored by TLC, reaction mixture was quenched with water and extracted with ethyl acetate. Combined organic layers were dried over anhydrous sodium sulphate, filtered and concentrated under reduced pressure to obtain the final product.

#### 4.1.1. 2-[1-(3-Nitro-phenyl)-1*H*-[1,2,3]triazol-4-ylmethylsulfanyl]-benzoxazole

Yellowish brown crystals; yield 85%; m.p. 210–211 °C; IR (KBr):  $\nu$  (cm<sup>-1</sup>) 3145, 3130, 1580, 1525, 1390, 924; <sup>1</sup>H NMR (400 MHz, DMSO):  $\delta$  4.80 (s, 2H), 7.31–7.37 (m, 2H), 7.66 (d, 1H, *J* = 1.6 Hz), 7.68 (d, 1H, *J* = 2.0 Hz), 7.88 (t, 1H, *J* = 8.0 Hz), 8.31 (dd, 1H, *J* = 1.2 and 8.0 Hz), 8.38 (dd, 1H, *J* = 1.2 and 8.0 Hz), 8.71 (t, 1H, *J* = 2.0 Hz), 9.08 (s, 1H); <sup>13</sup>C NMR (75 MHz, DMSO):  $\delta$  26.57, 110.06, 115.32, 118.45, 121.14, 123.23, 124.21, 124.46, 125.95, 130.93, 137.56, 141.66, 145.20, 148.85, 152.09, 163.96; ESI-MS: 354 (M+1)<sup>+</sup>; Anal. Calcd. for C<sub>16</sub>H<sub>11</sub>N<sub>5</sub>O<sub>3</sub>S: C, 54.38; H, 3.14; N, 19.82; S, 9.07. Found C, 54.39; H, 3.13; N, 19.83; S, 9.06.

#### 4.1.2. 2-[1-(4-Nitro-phenyl)-1*H*-[1,2,3]triazol-4-ylmethylsulfanyl]-benzoxazole

Yellowish brown crystals; yield 88%; m.p. 205–206 °C; IR (KBr):  $\nu$  (cm<sup>-1</sup>) 3155, 3127, 1598, 1533, 1376, 855; <sup>1</sup>H NMR (400 MHz, DMSO):  $\delta$  4.80 (s, 2H), 7.32–7.37 (m, 2H), 7.68 (dd, 2H, *J* = 1.6 and 7.2 Hz), 8.22 (d, 2H, *J* = 9.2 Hz), 8.43 (d, 2H, *J* = 6.9 Hz), 9.06 (s, 1H); <sup>13</sup>C NMR (75 MHz, DMSO):  $\delta$  26.42, 109.91, 118.33, 120.45, 121.32, 124.09, 124.34, 125.30, 140.93, 141.53, 144.99, 147.01, 151.89, 163.69; ESI-MS: 354 (M+1)<sup>+</sup>; Anal. Calcd. for C<sub>16</sub>H<sub>11</sub>N<sub>5</sub>O<sub>3</sub>S: C, 54.38; H, 3.14; N, 19.82; S, 9.07. Found C, 54.36; H, 3.12; N, 19.81; S, 9.05.

#### 4.1.3. 2-(1-Phenyl-1*H*-[1,2,3]triazol-4-ylmethylsulfanyl)-benzoxazole

White powder; yield 90%; m.p. 190–191 °C; IR (KBr):  $\nu$  (cm<sup>-1</sup>) 3165, 3130, 1530, 1520, 1354; <sup>1</sup>H NMR (400 MHz, DMSO):  $\delta$  4.78 (s, 2H), 7.31–7.37 (m, 2H), 7.49 (d, 1H, *J* = 7.6 Hz), 7.59 (d, 1H, *J* = 7.6 Hz), 7.89 (d, 2H, *J* = 8.0 Hz), 8.84 (s, 1H); <sup>13</sup>C NMR (75 MHz, DMSO):  $\delta$  26.56, 110.61, 118.43, 120.42, 120.55, 122.22, 123.59, 124.44, 124.60, 141.33, 141.63, 143.69, 147.31, 150.59, 163.78; ESI-MS: 309 (M+1)<sup>+</sup>; Anal. Calcd. for C<sub>16</sub>H<sub>12</sub>N<sub>4</sub>OS: C, 62.32; H, 3.92; N, 18.17; S, 10.40. Found C, 62.30; H, 3.91; N, 18.18; S, 10.39.

#### 4.1.4. 2-[1-(4-Ethyl-phenyl)-1*H*-[1,2,3]triazol-4-ylmethylsulfanyl]-benzoxazole

Yellowish white powder; yield 88%; m.p. 195–196 °C; IR (KBr):  $\nu$  (cm<sup>-1</sup>) 3250, 3140, 1490, 1433, 1256; <sup>1</sup>H NMR (400 MHz, DMSO):  $\delta$  1.20 (t, 3H), 2.67 (q, 2H, *J* = 6.8 Hz) 4.77 (s, 2H), 7.31–7.36 (m, 2H), 7.41 (d, 2H, *J* = 8.0 Hz), 7.67–7.69 (m, 2H), 7.77 (d, 2H, *J* = 8.4 Hz), 8.79 (s, 1H); <sup>13</sup>C NMR (75 MHz, DMSO):  $\delta$  16.86, 26.30, 109.41, 117.13, 121.25, 122.22, 124.09, 124.34, 125.30, 140.93, 141.53, 142.24, 144.99, 147.01, 152.65, 163.75; ESI-MS: 337 (M+1)<sup>+</sup>; Anal. Calcd. for C<sub>18</sub>H<sub>16</sub>N<sub>4</sub>OS: C, 64.26; H, 4.79; N, 16.65; S, 9.53. Found C, 64.27; H, 4.78; N, 16.64; S, 9.54.

#### 4.1.5. 2-[1-(4-Methoxy-phenyl)-1*H*-[1,2,3]triazol-4-ylmethylsulfanyl]-benzoxazole

White powder; yield 92%; m.p. 178–179 °C; IR (KBr):  $\nu$  (cm<sup>-1</sup>) 3165, 3116, 1468, 1433, 1356; <sup>1</sup>H NMR (400 MHz, DMSO):  $\delta$  3.82 (s, 3H), 4.76 (s, 2H), 7.11 (d, 2H, *J* = 9.2 Hz), 7.31–7.37 (m, 2H), 7.67–7.69 (m, 2H), 7.77 (d, 2H, *J* = 8.8 Hz), 8.73 (s, 1H); <sup>13</sup>C NMR (75 MHz, DMSO):  $\delta$  25.62, 52.34, 110.61, 117.23, 118.43, 120.34, 121.35, 125.14, 126.20, 141.93, 142.13, 143.39, 146.31, 152.89, 162.79; ESI-MS: 339 (M+1)<sup>+</sup>; Anal. Calcd. for C<sub>17</sub>H<sub>14</sub>N<sub>4</sub>O<sub>2</sub>S: C, 60.34; H, 4.17; N, 16.56; S, 9.48. Found C, 60.32; H, 4.18; N, 16.54; S, 9.49.

#### 4.1.6. 2-[1-(3-Chloro-phenyl)-1*H*-[1,2,3]triazol-4-ylmethylsulfanyl]-benzoxazole

Brown crystals; yield 94%; m.p. 203–204 °C; IR (KBr):  $\nu$  (cm<sup>-1</sup>) 3205, 3150, 1460, 1510, 1260; <sup>1</sup>H NMR (300 MHz, DMSO):  $\delta$  4.77 (s, 2H), 7.31–7.36 (m, 2H), 7.51–7.67 (m, 4H), 7.88 (d, 1H, *J* = 7.8 Hz), 8.00 (s, 1H), 8.91 (s, 1H); <sup>13</sup>C NMR (75 MHz, DMSO):  $\delta$  26.72, 110.04, 118.47, 120.75, 121.06, 124.13, 124.41, 128.84, 130.78, 135.51, 137.70, 141.76, 144.64, 152.10, 164.08; ESI-MS: 343 (M+1)<sup>+</sup>; Anal. Calcd. for C<sub>16</sub>H<sub>11</sub>ClN<sub>4</sub>OS: C, 56.06; H, 3.23; N, 16.34; S, 9.35. Found C, 56.04; H, 3.22; N, 16.33; S, 9.34.

#### 4.1.7. 2-[1-(4-Chloro-phenyl)-1*H*-[1,2,3]triazol-4-ylmethylsulfanyl]-benzoxazole

Brown powder; yield 90%; m.p. 196–197 °C; IR (KBr):  $\nu$  (cm<sup>-1</sup>) 3157, 1886, 1603, 1554, 1398, 924; <sup>1</sup>H NMR (300 MHz, DMSO):  $\delta$  4.77 (s, 2H), 7.33–7.36 (m, 2H), 7.64–7.69 (m, 4H), 7.93 (d, 2H, *J* = 9.0 Hz), 8.88 (s, 1H); <sup>13</sup>C NMR (75 MHz, DMSO):  $\delta$  26.65, 110.05, 118.41, 121.07, 121.72, 124.15, 124.41, 129.88, 134.59, 135.35, 141.71, 144.60, 152.07, 164.12; ESI-MS: 343 (M+1)<sup>+</sup>; Anal. Calcd. for C<sub>16</sub>H<sub>11</sub>ClN<sub>4</sub>OS:

**Table 4**

*In silico* ADME properties of the new ligands with respect to COX-2 protein.

Ligands	Molecular weight	Log S	PSA	Log P o/w
Celecoxib	381.372	-5.887	80.367	3.360
4	336.411	-4.836	54.094	4.149
9	387.253	-4.065	51.296	4.064
6	342.802	-4.865	53.289	4.055
14	336.411	-5.355	53.619	4.247
8	342.802	-5.051	48.343	4.338
2	353.355	-3.656	96.351	2.846
11	322.384	-5.057	47.668	4.270
13	326.347	-3.981	50.797	3.657
16	352.410	-3.647	57.710	3.797
10	326.347	-4.807	52.848	3.889
17	309.345	-3.204	62.352	2.794
18	343.790	-3.964	61.973	3.452
3	308.357	-4.502	50.048	3.876
5	338.383	-3.433	54.262	3.436
12	387.253	-5.332	48.931	4.475
1	353.355	-3.421	99.112	2.678
15	364.464	-6.505	55.411	5.103

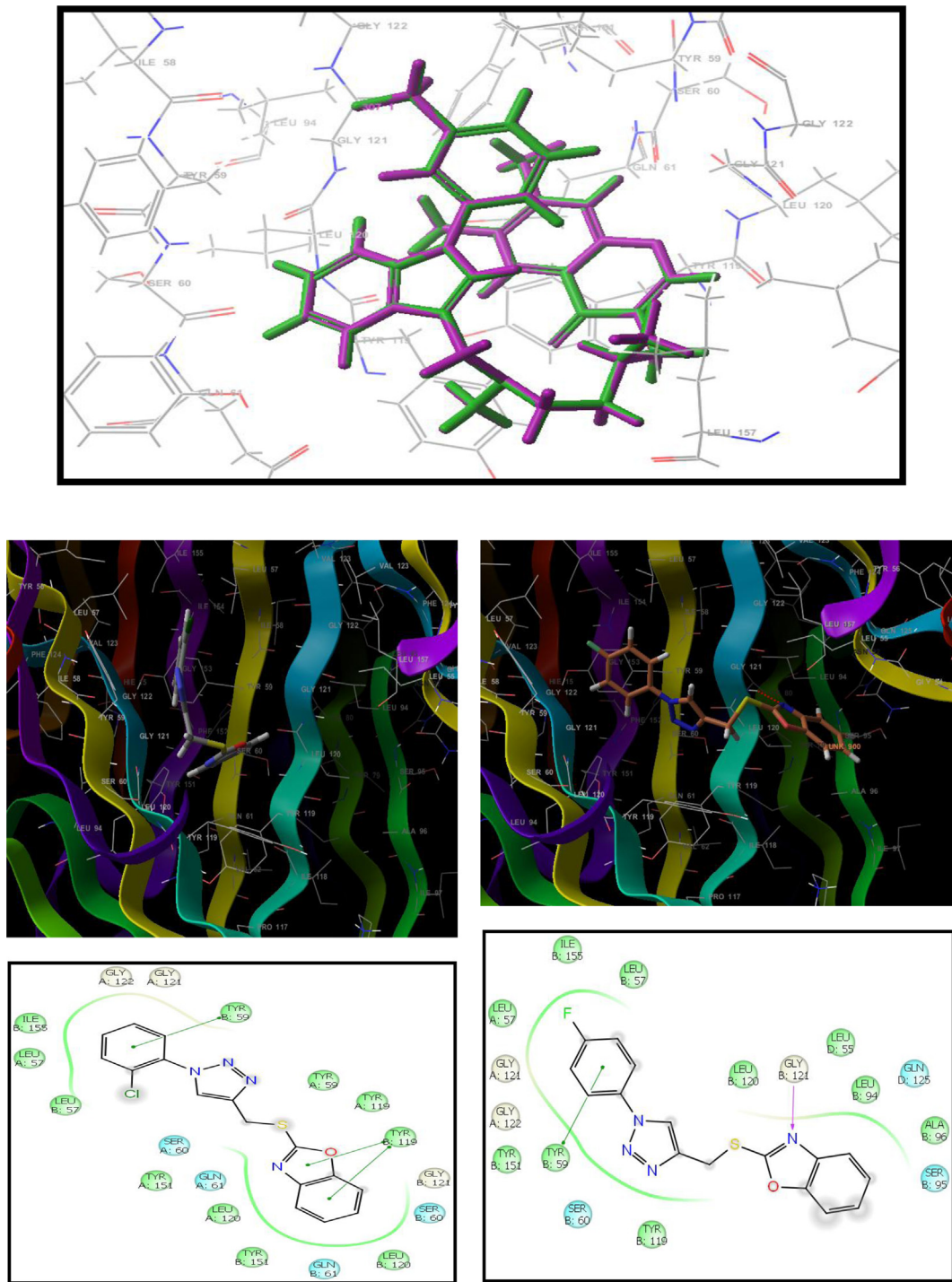


**Fig. 10.** a: The docked reference ligand used against TNF- $\alpha$  is shown. b: The *in silico* molecular docking structure of the compound **8** against TNF- $\alpha$  protein is shown. c: The *in silico* molecular docking structure of the compound **10** against TNF- $\alpha$  protein is shown.

C, 56.06; H, 3.23; N, 16.34; S, 9.35. Found C, 56.08; H, 3.21; N, 16.35; S, 9.33.

#### 4.1.8. 2-[1-(2-Chloro-phenyl)-1*H*-[1,2,3]triazol-4-ylmethylsulfanyl]-benzoxazazole

Yellow powder; yield 88%; m. p. 190–191 °C; IR (KBr):  $\nu$  (cm<sup>-1</sup>) 3139, 3115, 1556, 1500, 1456, 1237, 1137; <sup>1</sup>H NMR (300 MHz, DMSO):  $\delta$  4.79 (s, 2H), 7.32–7.35 (m, 2H), 7.53–7.75 (m, 6H), 8.60 (s, 1H); <sup>13</sup>C NMR (75 MHz, DMSO):  $\delta$  26.76, 110.01, 118.44, 124.06, 124.35,

125.08, 127.70, 127.89, 128.45, 130.74, 134.74, 141.79, 143.30, 152.06, 164.10; ESI-MS: 343 ( $M+1$ )<sup>+</sup>; Anal. Calcd. for C<sub>16</sub>H<sub>11</sub>ClN<sub>4</sub>OS: C, 56.06; H, 3.23; N, 16.34; S, 9.35. Found C, 56.04; H, 3.22; N, 16.33; S, 9.31.

#### 4.1.9. 2-[1-(4-Bromo-phenyl)-1*H*-[1,2,3]triazol-4-ylmethylsulfanyl]-benzoxazazole

Brown crystals; yield 86%; m.p. 212–213 °C; IR (KBr):  $\nu$  (cm<sup>-1</sup>) 3154, 3116, 1548, 1507, 1454, 1133, 1051; <sup>1</sup>H NMR (300 MHz, DMSO):

**Table 5**

*In silico* docking scores of the reference ligand 2AZ5 and 18 new ligands with respect TNF- $\alpha$ .

Ligands	G Score	Activity
2AZ5 Ligand	-7.10	-48.92
10	-6.77	-35.53
8	-6.38	-37.45
3	-6.10	-38.51
12	-5.99	-40.71
4	-5.88	-38.79
14	-5.71	-37.37
6	-5.68	-40.20
13	-5.66	-39.10
11	-5.63	-38.26
7	-5.60	-38.92
1	-5.43	-41.71
17	-5.42	-41.27
16	-5.15	-37.37
9	-5.14	-37.02
5	-5.06	-37.29
15	-5.06	-38.46
2	-5.05	-40.80
18	-4.68	-35.09

**Table 6**

*In silico* ADME properties of the ligands with respect to TNF- $\alpha$  protein.

Ligands	Molecular weight	Log S	PSA	Log P o/w
2AZ5 Ligand	547.619	-3.007	36.369	5.4
10	326.347	-5.184	56.864	4.028
8	342.802	-4.11	51.854	3.96
3	308.357	-4.828	55.745	3.788
12	387.253	-5.106	56.159	4.144
4	336.411	-4.183	54.454	4.042
14	336.411	-4.232	54.556	4.023
6	342.802	-5.474	56.372	4.335
13	326.347	-4.478	50.285	3.78
11	322.384	-4.998	56.358	3.998
7	342.802	-3.997	54.461	3.86
1	353.355	-4.834	95.451	3.2
17	309.345	-3.841	64.184	2.869
16	352.41	-5.485	60.916	4.393
9	387.253	-4.148	54.363	3.924
5	338.383	-3.255	62.608	3.43
15	364.464	-6.04	54.046	4.941
2	353.355	-3.795	99.345	2.734
18	343.79	-3.835	64.921	3.162

$\delta$  4.76 (s, 2H), 7.32–7.35 (m, 2H), 7.65–7.68 (m, 2H), 7.78 (d, 2H,  $J$  = 9.0 Hz), 7.86 (d, 2H,  $J$  = 9.0 Hz), 8.87 (s, 1H);  $^{13}\text{C}$  NMR (75 MHz, DMSO):  $\delta$  26.67, 110.06, 118.43, 120.95, 121.96, 122.49, 124.14, 124.41, 132.87, 135.86, 141.74, 144.69, 152.11, 164.15; ESI-MS: 387 (M+2)<sup>+</sup>,

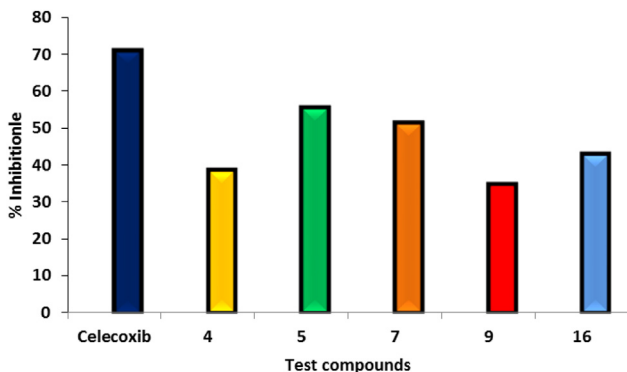


**Fig. 11.** *In vivo* antinociceptive activity of the active compounds by writhing test method.

388 (M+3)<sup>+</sup>; Anal. Calcd. for C<sub>16</sub>H<sub>11</sub>BrN<sub>4</sub>OS: C, 49.62; H, 2.86; N, 14.47; S, 8.28. Found C, 49.60; H, 2.87; N, 14.48; S, 8.27.

#### 4.1.10. 2-[1-(4-Fluoro-phenyl)-1*H*-[1,2,3]triazol-4-ylmethylsulfanyl]-benzoxazazole

White crystals; yield 92%; m.p. 194–195 °C; IR (KBr):  $\nu$  (cm<sup>-1</sup>) 3154, 3139, 1600, 1549, 1454, 1236, 1131;  $^1\text{H}$  NMR (300 MHz, DMSO):  $\delta$  4.77 (s, 2H), 7.30–7.36 (m, 2H), 7.40–7.46 (m, 2H), 7.66–7.69 (m, 2H), 7.90–7.94 (m, 2H), 8.81 (s, 1H);  $^{13}\text{C}$  NMR (75 MHz, DMSO):  $\delta$  26.74, 110.06, 116.53, 118.45, 121.25, 121.72, 122.55, 122.66, 124.13, 124.40, 141.80, 144.57, 152.15, 164.23; ESI-MS: 327 (M+1)<sup>+</sup>; Anal. Calcd. for C<sub>16</sub>H<sub>11</sub>FN<sub>4</sub>OS: C, 58.89; H, 3.40; N, 17.17; S, 9.83. Found C, 58.88; H, 3.39; N, 17.16; S, 9.84.

#### 4.1.11. 2-(1-o-Tolyl-1*H*-[1,2,3]triazol-4-ylmethylsulfanyl)-benzoxazazole

Yellowish white powder; yield 83%; m.p. 188–189 °C; IR (KBr):  $\nu$  (cm<sup>-1</sup>) 3144, 3124, 1555, 1505, 1379, 1135, 1100;  $^1\text{H}$  NMR (300 MHz, DMSO):  $\delta$  2.06 (s, 3H), 4.77 (s, 2H), 7.29–7.34 (m, 2H), 7.38 (d, 2H,  $J$  = 5.7 Hz), 7.45 (d, 2H,  $J$  = 5.7 Hz), 7.64–7.67 (m, 2H), 8.48 (s, 1H);  $^{13}\text{C}$  NMR (75 MHz, DMSO):  $\delta$  17.82, 26.83, 110.03, 118.43, 124.09, 124.37, 124.52, 125.95, 126.83, 129.87, 131.47, 133.56, 136.35, 141.79, 143.40, 152.07, 164.28; ESI-MS: 323 (M+1)<sup>+</sup>; Anal. Calcd. for C<sub>17</sub>H<sub>14</sub>N<sub>4</sub>OS: C, 63.33; H, 4.38; N, 17.38; S, 9.95. Found C, 63.32; H, 4.36; N, 17.39; S, 9.93.

#### 4.1.12. 2-[1-(2-Bromo-phenyl)-1*H*-[1,2,3]triazol-4-ylmethylsulfanyl]-benzoxazazole

Yellowish flakes; yield 86%; m.p. 202–203 °C; IR (KBr):  $\nu$  (cm<sup>-1</sup>) 3124, 3125, 1587, 1505, 1457, 1378, 1238, 1155;  $^1\text{H}$  NMR (300 MHz, DMSO):  $\delta$  4.78 (s, 2H), 7.29–7.36 (m, 2H), 7.50–7.58 (m, 2H), 7.61–7.67 (m, 3H), 7.86 (d, 1H,  $J$  = 7.8 Hz), 8.54 (s, 1H);  $^{13}\text{C}$  NMR (75 MHz, DMSO):  $\delta$  26.80, 110.03, 118.38, 118.47, 124.08, 124.36, 125.15, 128.14, 128.47, 131.15, 133.90, 141.82, 143.25, 152.07, 164.11; ESI-MS: 387 (M+2)<sup>+</sup>, 388 (M+3)<sup>+</sup>; Anal. Calcd. for C<sub>16</sub>H<sub>11</sub>BrN<sub>4</sub>OS: C, 49.62; H, 2.86; N, 14.47; S, 8.28. Found C, 49.63; H, 2.85; N, 14.46; S, 8.29.

#### 4.1.13. 2-[1-(2-Fluoro-phenyl)-1*H*-[1,2,3]triazol-4-ylmethylsulfanyl]-benzoxazazole

White powder; yield 90%; m.p. 187–188 °C; IR (KBr):  $\nu$  (cm<sup>-1</sup>) 3182, 3170, 1595, 1379, 1047;  $^1\text{H}$  NMR (300 MHz, DMSO):  $\delta$  4.81 (s, 2H), 7.31–7.36 (m, 2H), 7.44 (d, 1H,  $J$  = 7.5 Hz), 7.52–7.59 (m, 2H), 7.67–7.69 (m, 2H), 7.83 (t, 1H,  $J$  = 7.8 Hz), 8.64 (s, 1H);  $^{13}\text{C}$  NMR (75 MHz, DMSO):  $\delta$  26.72, 111.02, 116.49, 118.47, 120.36, 121.27, 121.70, 122.54, 122.65, 124.10, 124.42, 141.82, 144.55, 152.18, 164.20; ESI-MS: 327 (M+1)<sup>+</sup>; Anal. Calcd. for C<sub>16</sub>H<sub>11</sub>FN<sub>4</sub>OS: C, 58.89; H, 3.40; N, 17.17; S, 9.83. Found C, 58.87; H, 3.38; N, 17.18; S, 9.82.

#### 4.1.14. 2-[1-(3,4-Dimethyl-phenyl)-1*H*-[1,2,3]triazol-4-ylmethylsulfanyl]-benzoxazazole

Yellow powder; yield 88%; m.p. 211–212 °C; IR (KBr):  $\nu$  (cm<sup>-1</sup>) 3145, 3118, 1501, 1454, 1133, 1098, 1045;  $^1\text{H}$  NMR (300 MHz, DMSO):  $\delta$  2.27 (s, 3H), 2.30 (s, 3H), 4.76 (s, 2H), 7.30–7.38 (m, 3H), 7.55 (d, 1H,  $J$  = 8.1 Hz), 7.67 (d, 3H,  $J$  = 6.6 Hz), 8.72 (s, 1H);  $^{13}\text{C}$  NMR (75 MHz, DMSO):  $\delta$  19.43, 19.86, 26.85, 110.04, 117.92, 118.45, 121.12, 121.81, 124.07, 124.36, 130.58, 134.84, 137.64, 138.34, 141.83, 144.03, 152.11, 164.33; ESI-MS: 337 (M+1)<sup>+</sup>; Anal. Calcd. for C<sub>18</sub>H<sub>16</sub>N<sub>4</sub>OS: C, 64.26; H, 4.79; N, 16.65; S, 9.53. Found C, 64.24; H, 4.78; N, 16.64; S, 9.51.

#### 4.1.15. 2-[1-(4-Tert-Butyl-phenyl)-1*H*-[1,2,3]triazol-4-ylmethylsulfanyl]-benzoxazazole

White powder; yield 88%; m.p. 193–195 °C; IR (KBr):  $\nu$  (cm<sup>-1</sup>) 3154, 3141, 1555, 1520, 1453, 1378, 1133;  $^1\text{H}$  NMR (300 MHz, DMSO):  $\delta$  1.31 (s, 9H), 4.77 (s, 2H), 7.32–7.36 (m, 2H), 7.58 (d, 2H,  $J$  = 8.7 Hz),

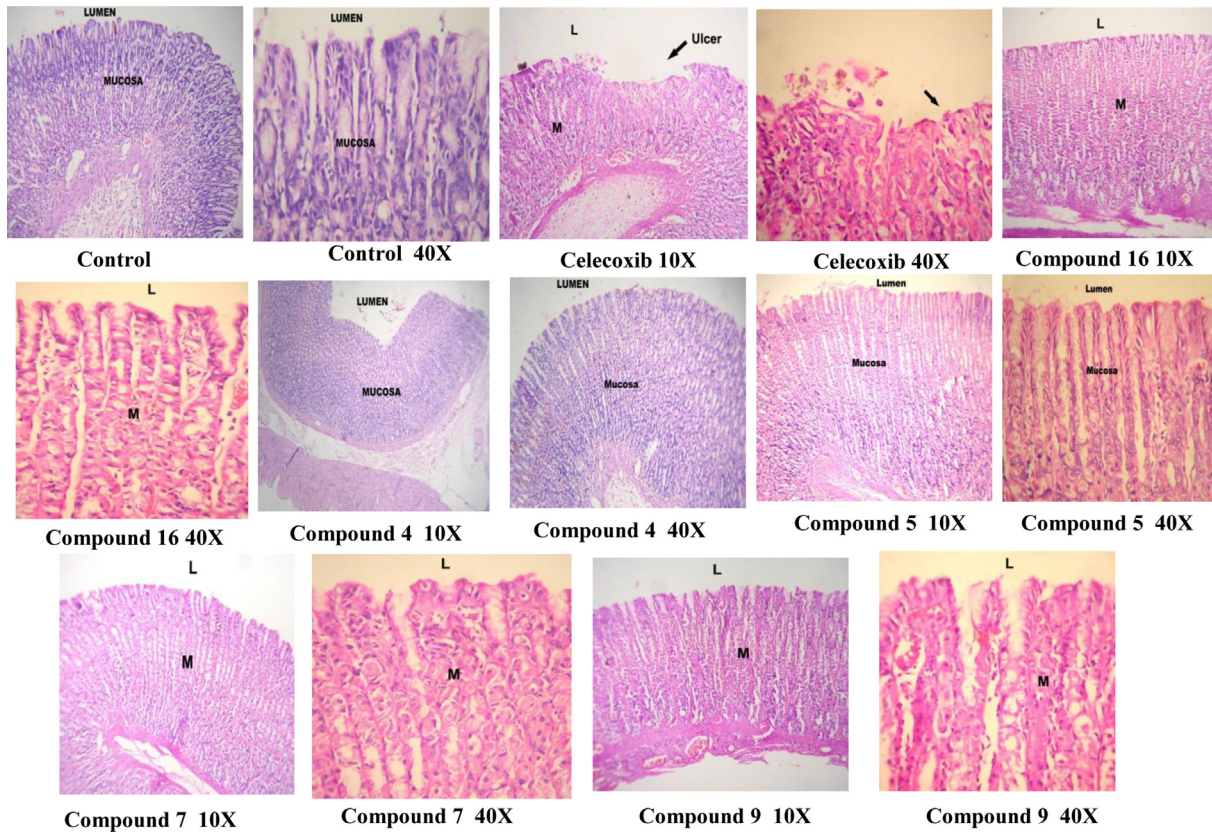


**Fig. 12.** The histopathology report of the active compounds is shown.

7.65–7.69 (m, 2H), 7.77 (d, 2H,  $J = 8.7$  Hz), 8.77 (s, 1H);  $^{13}\text{C}$  NMR (75 MHz, DMSO):  $\delta$  26.83, 31.23, 34.76, 110.04, 118.44, 120.33, 121.15, 124.08, 124.37, 126.59, 134.50, 141.81, 144.11, 152.10, 152.22, 164.30; ESI-MS: 365 ( $M+1$ ) $^+$ ; Anal. Calcd. for  $\text{C}_{20}\text{H}_{20}\text{N}_4\text{OS}$ : C, 65.91; H, 5.53; N, 15.37; S, 8.80. Found C, 65.90; H, 5.54; N, 15.36; S, 8.81.

#### 4.1.16. 2-[1-(4-Ethoxy-phenyl)-1*H*-[1,2,3]triazol-4-ylmethylsulfanyl]-benzoxazole

White powder; yield 85%; m. p. 186–187 °C; IR (KBr):  $\nu$  (cm $^{-1}$ ) 3155, 3143, 1522, 1498, 1457, 1390, 1251;  $^1\text{H}$  NMR (300 MHz, DMSO):  $\delta$  1.34 (t, 3H,  $J = 6.6$  Hz), 4.09 (q, 2H,  $J = 6.9$  Hz), 4.76 (s, 2H),

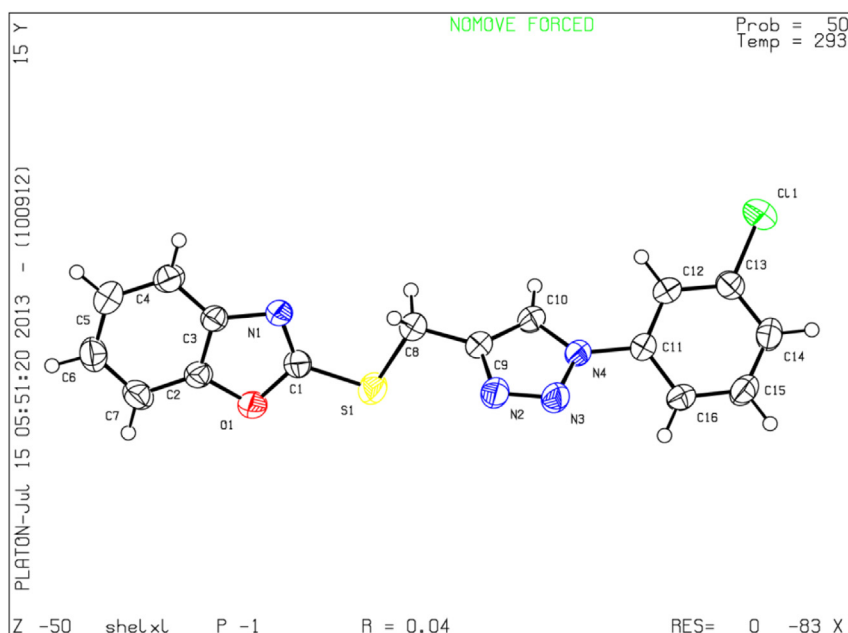


**Fig. 13.** The X-ray crystallographic structure of the compound 2-[1-(3-Chloro-phenyl)-1*H*-[1,2,3]triazol-4-ylmethylsulfanyl]-benzoxazole(**6**) is shown.

7.09 (d, 2H,  $J = 9.0$  Hz), 7.30–7.38 (m, 2H), 7.66–7.68 (m, 2H), 7.75 (d, 2H,  $J = 8.7$  Hz), 8.77 (s, 1H);  $^{13}\text{C}$  NMR (75 MHz, DMSO):  $\delta$  14.69, 26.84, 63.91, 110.04, 115.25, 118.45, 121.24, 122.24, 124.07, 124.36, 130.22, 132.91, 141.82, 144.04, 152.11, 164.32; ESI-MS: 353 ( $M+1$ ) $^+$ ; Anal. Calcd. for  $\text{C}_{18}\text{H}_{16}\text{N}_4\text{O}_2\text{S}$ : C, 61.35; H, 4.58; N, 15.90; S, 9.10. Found C, 61.33; H, 4.57; N, 15.89; S, 9.11.

#### 4.1.17. 2-(1-Pyridin-3-yl-1*H*-[1,2,3]triazol-4-ylmethylsulfanyl)-benzoxazole

Brown powder; yield 84%; m.p. 193–194 °C; IR (KBr):  $\nu$  (cm $^{-1}$ ) 3155, 3144, 1555, 1505, 1453, 1131, 1095;  $^1\text{H}$  NMR (300 MHz, DMSO):  $\delta$  4.78 (s, 2H), 7.30–7.33 (m, 2H), 7.59–7.66 (m, 3H), 8.29 (d, 1H,  $J = 7.8$  Hz), 8.66 (d, 1H,  $J = 3.9$  Hz), 8.29 (s, 1H), 9.10 (s, 1H);  $^{13}\text{C}$  NMR (75 MHz, DMSO):  $\delta$  26.18, 109.61, 118.01, 120.97, 123.75, 123.83, 124.02, 127.63, 133.06, 141.16, 141.24, 144.31, 149.49, 151.59, 163.49; ESI-MS: 353 ( $M+1$ ) $^+$ ; Anal. Calcd. for  $\text{C}_{15}\text{H}_{11}\text{N}_5\text{OS}$ : C, 58.24; H, 3.58; N, 22.64; S, 10.37. Found C, 58.22; H, 3.57; N, 22.62; S, 10.36.

#### 4.1.18. 2-[1-(2-Chloro-pyridin-3-yl)-1*H*-[1,2,3]triazol-4-ylmethylsulfanyl]-benzoxazole

Yellow powder; yield 85%; m.p. 186–187 °C; IR (KBr):  $\nu$  (cm $^{-1}$ ) 3154, 3132, 1571, 1497, 1457, 1135, 1100;  $^1\text{H}$  NMR (300 MHz, DMSO):  $\delta$  4.80 (s, 2H), 7.33–7.35 (m, 2H), 7.65–7.71 (m, 3H), 8.21 (d, 1H,  $J = 7.8$  Hz), 8.63 (d, 1H,  $J = 3.6$  Hz), 8.67 (s, 1H);  $^{13}\text{C}$  NMR (75 MHz, DMSO):  $\delta$  26.63, 110.03, 118.47, 123.33, 124.16, 124.42, 124.90, 131.97, 135.84, 141.75, 143.99, 144.81, 150.20, 152.09, 163.94; ESI-MS: 344 ( $M+1$ ) $^+$ ; Anal. Calcd. for  $\text{C}_{15}\text{H}_{10}\text{ClN}_5\text{OS}$ : C, 52.40; H, 2.93; N, 20.37; S, 9.33. Found C, 52.39; H, 2.94; N, 20.35; S, 9.31.

## 4.2. Pharmacology

### 4.2.1. Animals

Albino Wistar rats of either sex (150–200 g) were obtained from Central Animal House, Hamdard University, New Delhi. The animals were kept in cages at the room temperature and fed with food and water ad libitum. Fourteen hours before the start of the experiment the animals were sent to lab and fed only with water ad libitum. The experiments were performed in accordance with the rules of Institutional Animals Ethics Committee (registration number 173-CPCSEA).

### 4.2.2. Chemicals

Celecoxib, carrageenan, potassium chloride and carboxymethylcellulose along with the other chemicals used in the different experiments were purchased from Sigma–Aldrich Chemicals Pvt. Limited, Bangalore, India.

### 4.2.3. Anti-inflammatory activity

The synthesized compounds were tested for their *in vivo* anti-inflammatory activity using carrageenan-induced hind paw edema method. The rat paw edema was induced by subcutaneous injection of 0.1 ml of 1% freshly prepared saline solution [41] of carrageenan into the right hind paw of rats. The standard drug, celecoxib (0.05 mmol/kg) was given orally as a positive control. The control group was administered orally with 0.9% of 0.1 ml of saline solution only. The test groups were administered orally with equimolar dosage of the synthesized compounds as the standard drug, 1 h before the administration of carrageenan. The paw volumes were measured using plethysmometer [42] at interval of 3 h and 5 h.

### 4.2.4. Measurement of IL-1 $\beta$ , TNF- $\alpha$ and COX-2

Levels of the proinflammatory cytokines (IL-1 $\beta$  and TNF- $\alpha$ ) [43] and COX-2 [44] in the serum have been determined by using commercially available ELISA kits (eBioscience and Cayman, USA).

Assays have been performed in duplicate in accordance to the manufacturer's guidelines. Cytokine concentrations were expressed as picograms of antigen per millilitre of protein.

### 4.2.5. COX-2 gene expression study

**4.2.5.1. Cell culture experiments.** HeLa cells (ATCC) were seeded in 24 well plate, 24 h before the treatment in DMEM containing 10% calf serum (Invitrogen). After 24 h cells were treated with compounds **4** & **9** (10  $\mu\text{M}$ ) and the standard drug celecoxib (10  $\mu\text{M}$ ) as positive control and DMSO as negative control followed by 24 h of incubation of cells in  $\text{CO}_2$  incubator at 37 °C and 5%  $\text{CO}_2$ .

**4.2.5.2. RNA extraction, reverse transcription and gene expression analysis.** After 24 h cells were scrapped and collected in 1.5 ml micro centrifuge tubes. The total RNA was isolated by TRI Reagent® (Molecular Research Centre). RNA quantity and quality was determined on a NanoDrop ND-2000c spectrophotometer and integrity was checked on a 1.5% agarose gel. Total RNA (1  $\mu\text{g}$ ) was used to generate cDNA using an EZfirst strand cDNA synthesis kit for RT (reverse transcription)–PCR (Biological Industries). Primers for real-time PCR were designed for COX-2 and GAPDH using the Pearl Primer software and are listed in Table 7.

Reactions were run at 95 °C for 10 min followed by 40 cycles of 95 °C for 15 s and 60 °C for 1 min. Real-time PCR was performed on an ABI Prism 7300 Sequence Detection System (Applied Biosystems) using the SYBR Green PCR Master Mix (Applied Biosystems). PCR was performed in triplicate and was repeated two times for each gene and each sample. Relative transcript quantities were calculated using the Ct method with GAPDH as the endogenous reference gene.

### 4.2.6. Estimation of thiobarbituric acid reactive substances (TBARS)

The assay of TBARS was done according to earlier method [45] adapted to microtiter plates by bringing the final volume to 150  $\mu\text{L}$ . In brief, hind paw tissue homogenate was prepared in 0.15 M KCl (5% w/v homogenate) and aliquots of 30  $\mu\text{L}$  were incubated for 0 °C and 37 °C for 1 hr. Subsequently, 60  $\mu\text{L}$  of 28% w/v TCA was added and the volume was made up to 150  $\mu\text{L}$  by adding 60  $\mu\text{L}$  of distilled water followed by centrifugation at 3000  $\times g$  for 10 min. The supernatant (125  $\mu\text{L}$ ) was taken and colour was developed by addition of 25  $\mu\text{L}$  of 1% w/v TBA dissolved in 0.05 N NaOH and kept in boiling water bath for 15 min. The absorbance was read at 532 nm in a plate reader (Bio-Rad, U.S.A.). The results are expressed in  $\mu\text{moles}$  of TBARS formed/hr/g tissue using a molar extinction coefficient of  $1.56 \times 10^5 \text{ M}^{-1} \text{ cm}^{-1}$ .

### 4.2.7. Reduced glutathione (GSH)

GSH level was measured using the method described earlier [46]. Homogenized hind paw tissue (10% w/v in phosphate buffer pH 7.4) was deproteinized by adding an equal volume of 10% TCA and was allowed to stand at 4 °C for 2 h. The contents were centrifuged at 2000  $\times g$  for 15 min. 50  $\mu\text{L}$  supernatant was added to 200  $\mu\text{L}$  of 0.4 M Tris buffer (pH 8.9) containing 0.02 M EDTA (pH 8.9) followed by the addition 20  $\mu\text{L}$  of 0.01 M DTNB. The absorbance was read in a microplate reader at 412 nm and results are expressed as

**Table 7**

Primer list used in the COX gene expression study.

Gene	Primer	Sequence (5' to 3')
COX2	Forward Primer	CTTCAACTCCTACATACTCCC
	Reverse Primer	GTTTGCTCACAGATTTCAG
GAPDH	Forward Primer	CATTCCTGGTATGACAACGA
	Reverse Primer	GTCTACATGGCAACTGTGAG

$\mu\text{g GSH/g tissue}$  using a molar extinction coefficient of  $13.6 \times 10^3 \text{ M}^{-1} \text{ cm}^{-1}$ .

#### 4.2.8. Measurement of nitric oxide (NO) level

Animals were sacrificed and their hind paw tissues were washed with PBS (pH 7.4) and placed on ice as described earlier [47]. 50  $\mu\text{L}$  of the sample was added to 100  $\mu\text{L}$  of Griess reagent and reaction mixture was incubated for about 5–10 min at room temperature and protected from light. The optical density was measured at 540 nm in microplate reader according to the reagent manufacturer's protocol. Calculations were done after generating a standard curve for sodium nitrite in the same buffer as used for preparation of homogenate.

#### 4.2.9. Antinociceptive activity

**4.2.9.1. Writhing test.** The writhing test in mice was carried out using the method of Koster [48]. The writhes were induced by intraperitoneal injection of 0.6% acetic acid (v/v) (80 mg/kg). The standard drug i.e. celecoxib was given orally at a dose 0.05 mmol/kg of body weight. The test compounds were administered orally at an equimolar dosage to groups of six animals each, 30 min before chemical stimulus. The numbers of muscular contractions were counted over a period of 20 min after acetic acid injection. The data represents the total number of writhes observed during 20 min and is expressed as writhing numbers.

#### 4.3. Ulcerogenic activity

The compounds having anti-inflammatory and antinociceptive activities comparable with celecoxib were further tested for their ulcerogenic risk evaluation [49]. This was done at three times higher dose in comparison to the dose used for anti-inflammatory activity, i.e. 0.15 mmol/kg body weight of celecoxib and the test compounds were used. Each group had three animals which were later sacrificed after 5 h of oral drug administration. When compared with celecoxib, these compounds did not cause any gastric ulceration and disruption of gastric epithelial cells at the above mentioned oral dose. Hence the gastric tolerance of these compounds towards the gastric mucosa was better than that of celecoxib.

#### 4.4. Molecular docking studies on COX-2

Crystallized structure of COX-2 protein with reported ligand (celecoxib) was considered for the docking studies. For this purpose we shortlisted Protein 3LN1 from Protein Data Bank as this includes celecoxib drug selectivity bound to binding site of COX. The structure of protein COX-2 along with celecoxib (3LN1) was retrieved from the Protein Data Bank (PDB). First protein structure of 3LN1 was imported in Schrodinger using Protein Preparation Wizard. This wizard was used to optimize and minimize the protein structure which involves removing undesirable water molecules and other defects in the target protein. Finally a low energy and structurally correct target protein was achieved. This minimized protein was used for further docking analysis. As the target protein has already the site for celecoxib, the grid was generated by selecting the celecoxib ligand as the reference ligand. Finally the grid was validated and was used for further docking with new unknown molecules to predict their docking score. Chemical structures were drawn in maestro and geometrically refined by LigPrep module for Ligand preparation. In this module 2-D structures were converted into 3-D structures, which were further subjected to OPLS-2005 force field to generate single low energy 3-D structure for each input structure. During this step chiralities were maintained. Docking was carried using Glide software. It was

carried using Extra precision and write XP descriptor information. This generates favourable ligand poses which were further screened through filters to examine the spatial fit of the ligands in the active site. Ligand poses which pass through initial screening are subjected to evaluation and minimization of grid approximation. Scoring is then carried on energy minimized poses to generate Glide score.

#### 4.5. Molecular docking studies on TNF- $\alpha$

Crystallized structure of 2AZ5 was chosen from Protein Data Bank and used as target for molecular docking studies. 2AZ5 structure was reported with the specific ligand celecoxib which inhibits it. 2AZ5 structure was imported in Schrodinger using Protein Preparation Wizard. Missing hydrogen and other atoms were added using prime interface. Undesired water molecules were removed. The protein was then optimized and minimized to give low energy and structurally correct target protein. As the target protein had already the site for reference ligand, the grid was generated by selecting the ligand as the reference ligand. Finally the grid was validated and was used for further docking with new unknown ligands to predict their docking score. Chemical structures were drawn in maestro and geometrically refined by LigPrep module. In this module 2-D structures were converted into 3-D structures, which were further subjected to OPLS-2005 force field to generate single low energy 3-D structure for each input structure. During this step chiralities were maintained. Docking was carried out using Glide software using Extra precision and write XP descriptor information. This generates favourable ligand poses which were further screened through the filters to examine spatial fit of the ligand into the active site. Ligand poses which pass through initial screening are subjected to evaluation and minimization of grid approximation. Scoring is then carried on energy minimized poses to generate Glide score.

#### Acknowledgements

The authors thank Dr. G.N. Qazi, Vice-Chancellor, Jamia Hamdard for providing necessary facilities to the Department of Chemistry. One of the authors (SH) is also thankful to Council of Scientific and Industrial Research (CSIR), New Delhi for the award of senior research fellowship.

#### Appendix A. Supplementary data

Supplementary data related to this article can be found at <http://dx.doi.org/10.1016/j.ejmech.2014.05.012>.

#### References

- [1] M.M. Wolfe, D.R. Lichtenstein, G. Singh, N. Engl. J. Med. 340 (1999) 1888–1899.
- [2] M.C. Allison, A.G. Howatson, C.J. Torrance, F.D. Lee, R.I. Russell, N. Engl. J. Med. 327 (1992) 749–754.
- [3] R. Karima, S. Matsumoto, H. Higashi, K. Matsushima, Mol. Med. Today 5 (1999) 123–132.
- [4] G. Schlag, H. Redl, S. Hallstrom, Resuscitation 21 (1991) 137–180.
- [5] H. Birkedal-Hansen, J. Periodont. Res. 28 (1993) 500–510.
- [6] S. Shafi, M.M. Alam, N. Mulakayala, C. Mulakayala, G. Vanaja, A.M. Kalle, R. Pallu, M.S. . Alam, Eur. J. Med. Chem. 49 (2012) 324–333.
- [7] J. Susperregui, M. Bayle, J.M. Léger, G. Délérés, J. Organ. Mett. Chem. 556 (1998) 105–110.
- [8] P. Kohli, S.D. Srivastava, S.K. Srivastava, J. Chin. Chem. Soc. 54 (2007) 1003–1010.
- [9] V. Şunel, M. Popa, C.L. Dumitriu, A. Ciobanu, I. Bunia, A.A. Popa, React. Funct. Polym. 65 (2005) 367.
- [10] S.M. Rida, F.A. Ashour, S.A.M. El-Hawash, M.M. ElSemary, M.H. Badr, M.A. Shalaby, Eur. J. Med. Chem. 40 (2005) 949–959.

- [11] A.A. Hare, L. Leng, S. Gandavi, X. Du, Z. Cournia, W.L. Jorgensen, *Bioorg. Med. Chem. Lett.* 20 (2010) 5811–5814.
- [12] J. Vinsova, K. Cermakova, A. Tomeckova, M. Ceckova, J. Jampilek, J. Kunes, M. Dolezal, F. Staud, *Bioorg. Med. Chem.* 14 (2006) 5850–5865.
- [13] Z. Tian, D.J. Plata, S.J. Wittenberger, A.V. Bhatia, *Tetrahedron Lett.* 46 (2005) 8341–8343.
- [14] (a) D.R. Buckle, C.J.M. Rockell, *J. Chem. Soc. Perkin Trans.* (1982) 627–630; (b) D.R. Buckle, D.J. Outred, C.J.M. Rockell, H. Smith, B.A. Spicer, *J. Med. Chem.* 26 (1983) 251–254.
- [15] M.D. Chen, S.J. Lu, G.P. Yuag, S.Y. Yang, X.L. Du, *Heterocyclic Comm.* 6 (2000) 421–426.
- [16] E.A. Shеремет, R.I. Tomanov, E.V. Trukhin, V.M. Berestovitskaya, *Russ. J. Org. Chem.* 40 (2004) 594–595.
- [17] A. Allais, J. Meier, (*Roussel-UCLAF*) Ger. Offen. (1969) 1815467.
- [18] K.M. Banu, A. Dinakar, C. Ananthanarayanan, *Ind. J. Pharm. Sci.* 4 (1999) 202–205.
- [19] R. Meier, EP. 199262; Eidem, US. 4789680, 1986.
- [20] A. Passannanti, P. Diana, P. Barraja, F. Mingoia, A. Lauria, G. Cirrincione, *Heterocycles* 48 (1998) 1229–1235.
- [21] M. Jilino, F.G. Stevens, *J. Chem. Soc. Perkin Trans. 1* (1998) 1677–1684.
- [22] G.D. Diana, J.J. Nitz, EP. 566199, (1993).
- [23] H.G. Kim, E.H. Han, W.S. Jang, J.H. Choi, T. Khanal, B.H. Park, T.P. Tran, Y.C. Chung, H.G. Jeong, *Food Chem. Toxicol.* 50 (2012) 2342–2348.
- [24] M. Duwiejua, I.J. Zeitlin, P.G. Waterman, J. Chapman, G.J. Mhango, G.J. Provan, *Planta. Med.* 59 (1993) 12–16.
- [25] Y. Juarranz, C. Abad, C. Martinez, A. Arranz, I. Gutierrez-Canas, F. Rosignoli, R.P. Gomariz, J. Leceta, *Arthritis Res. Ther.* 7 (2005) R1034–R1045.
- [26] R.A. Mothana, *Food. Chem. Toxicol.* 49 (2011) 2594–2599.
- [27] G. Schett, C. Stach, J. Zwerina, R. Voll, B. Manger, *Arthritis. Rheum.* 58 (2008) 2936–2948.
- [28] K. Bauerova, S. Ponist, D. Mihalova, F. Drafi, V. Kuncirova, *Interdiscip. Toxicol.* 4 (2011) 33–39.
- [29] R.T. Narendhirakannan, T.P. Limmy, *Immunopharmacol. Immunotoxicol.* 34 (2011) 326–336.
- [30] M.Q. Hassan, R.A. Hadi, Z.S. Al-Rawi, V.A. Padron, S.J. Stohs, *J. Appl. Toxicol.: JAT* 21 (2001) 69–73.
- [31] M.M. Khan, T. Ishrat, A. Ahmad, M.N. Hoda, M.B. Khan, G. Khujwaja, P. Srivastava, S.S. Raza, F. Islam, S. Ahmad, *Chem. Biol. Interact.* 183 (2010) 255–263.
- [32] A. Kiziltunc, S. Cogalgil, L. Cerrahoglu, *Scand. J. Rheumatol.* 27 (1998) 441–445.
- [33] W.G. Seo, H.O. Pae, G.S. Oh, K.Y. Chai, T.O. Kwon, Y.G. Yun, N.Y. Kim, H.T. Chung, *J. Ethnopharmacol.* 76 (2001) 59–64.
- [34] M. Shukla, K. Gupta, Z. Rasheed, K.A. Khan, T.M. Haqqi, *J. Inflamm.* 5 (2008) 9.
- [35] S. Umar, A. Kumar, M. Sajad, J. Zargan, M.M. Ansari, S. Ahmad, C.K. Katiyar, H.A. Khan, *Rheumatol. Int.* 33 (2013) 653–657.
- [36] Xcalibur CCD System, Oxford Diffraction Ltd, Abingdon, Oxfordshire, England, 2007.
- [37] R.C. Clark, J.S. Reid, *Acta. Crystallogr. A51* (1995) 887–897.
- [38] CrysAlisPro (versions 1.171.34.49), Oxford Diffraction Ltd, Abingdon, Oxfordshire, England.
- [39] G.M. Sheldrick, *Acta. Crystallogr. A64* (2008) 112–122.
- [40] L.J. Farrugia, *J. Appl. Cryst.* 45 (2012) 849–854.
- [41] C.A. Winter, E.A. Risley, G.W. Nuss, *Proc. Soc. Exp. Biol. Med.* 111 (1962) 544–547.
- [42] S.H. Ferreira, *J. Pharm. Pharmacol.* 31 (1979) 648.
- [43] U. Sadiq, H. Abu, U. Khalid, S. Mir, A. Niyaz, A. Sayeed, K.K. Chandra, A.K. Haider, *Cell. Immunol.* 284 (2013) 51–59.
- [44] L.J. Crofford, R.L. Wilder, A.P. Ristimaki, E.F. Remmers, H.R. Epps, T. Hla, *J. Clin. Invest.* 93 (1994) 1095–1101.
- [45] H.G. Utley, F. Bernheim, P. Hochstein, *Arch. Biochem. Biophys.* 118 (1967) 29–32.
- [46] J. Sedlak, R.H. Lindsay, *Anal. Biochem.* 25 (1968) 192–205.
- [47] S. Umar, J. Zargan, K. Umar, S. Ahmad, C.K. Katiyar, H.A. Khan, *Chem. Biol. Interact.* 197 (2012) 40–46.
- [48] R. Koster, M. Anderson, E.J. Beer, *Fed. Proc.* 18 (1959) 412–416.
- [49] S. Haider, S. Nazreen, M.M. Alam, H. Hamid, M.S. Alam, *J. Ethnopharmacol.* 143 (2012) 236–240.